 https://doi.org/10.3311/PPtr.39763


**Periodica Polytechnica Transportation Engineering**, 53(3), pp. 334–346, 2025

# Performance of PMMA and SBS Modified Asphalt Mixtures in Railway Supplementary Layers and Road Pavements

Furkan Kaya[1], Şevket Aslan[1], Mohammad Fahad[2,3], Klaudia Madarász[2,3], Szabolcs Rosta[2,3], Richárd Nagy[2,3], Szabolcs Fischer[2,3*]

[1] Department of Civil Engineering, Faculty of Engineering, Erciyes University, TR-38030, Melikgazi, Kayseri, Türkiye
[2] Department of Transport Infrastructure and Water Resources Engineering, Széchenyi István University, Egyetem Tér 1, H-9026 Győr, Hungary
[3] Vehicle Industry Research Center, Széchenyi István University, Egyetem Tér 1, H-9026 Győr, Hungary
[*] Corresponding author, e-mail: fischersz@sze.hu

Received: 31 December 2024, Accepted: 03 April 2025, Published online: 16 April 2025

**Abstract**

The use of recycled waste elastic materials provides a cost-effective and environmentally friendly option for further modifying the performance of asphalt mixtures. Therefore, the effects of different proportions of (PMMA) polymethyl methacrylate derived from waste plastic material were evaluated using the Indirect Tensile Strength Test (ITST) of lab-prepared specimens. Since numerous methods of modifying the conventional asphalt binder are available, in this research, the virgin binder was modified with 1%, 2%, 3%, 4% and 5% PMMA for evaluating optimum performance proportions in terms of Marshall stability and ITST of asphalt mixtures. Furthermore, stiffness modulus tests were performed at frequency values of 1.2 Hz, 1.9 Hz, 3.9 Hz and 5 Hz. The effect of the loading rate from 10 MPa/s to 70 MPa/s was evaluated with an increment of 10 MPa/s for all proportions. Moreover, finite element modeling was performed using the data obtained from dynamic modulus tests with modified Burger's Logit model for evaluation of rutting progression. Results show improved performance of asphalt mixtures with the addition of PMMA, leading to variation in properties including penetration, softening point, Marshall stability and rutting resistance. It is recommended to use 5% PMMA for increased indirect tensile strength, Marshall stability, rutting and fatigue damage resistance.

**Keywords**

railway supplementary layer, road pavement, asphalt support layer, polymer modification, ABAQUS, polymethyl methacrylate, asphalt

## 1 Introduction

Road pavements and railway superstructures, as well as their sublayers and substructures are the backbone of transportation networks, ensuring efficient movement of goods and people. These critical systems face increasing traffic loads, driving advancements in engineering. The performance and durability of transportation infrastructure depend heavily on the materials used, especially under repetitive loading conditions. Among these materials, crushed stone aggregates significantly influence the structural integrity of road pavements and railway tracks (Ézsiás et al., 2024). In railway systems, ballasted tracks serve as a critical component requiring specialized designs to mitigate settlement caused by dynamic loads (Fischer, 2025).

To further enhance reliability, predictive maintenance systems leveraging big data and artificial intelligence have revolutionized track geometry management (Nagy et al., 2024; Vitković et al., 2024). At the same time, optimizing logistics and resource management has become a cornerstone for achieving both efficiency and minimizing environmental impact during construction and maintenance (Saukenova et al., 2022; Volkov et al., 2020). These general advancements set the stage for specific innovations, such as the integration of recycled materials like polymethyl methacrylate (PMMA) into asphalt mixtures, to improve infrastructure resilience. Such approaches, improve resistance to fatigue and deformation.

PMMA-modified asphalt mixtures enhance viscoelastic properties, including stiffness modulus and rutting resistance under varying loads and climates (Du et al., 2020; Fahad et al., 2021). Advanced finite element modeling further supports resilient infrastructure design by predicting behavior under complex operational conditions in road

**Cite this article as:** Kaya, F., Aslan, S., Fahad, M., Madarász, K., Rosta, S., Nagy, R., Fischer, S. (2025) "Performance of PMMA and SBS Modified Asphalt Mixtures in Railway Supplementary Layers and Road Pavements", Periodica Polytechnica Transportation Engineering, 53(3), pp. 334–346.
https://doi.org/10.3311/PPtr.39763

pavements (Huang et al., 2020; Majidi Shad et al., 2022), as well as in railway systems (Kuchak et al., 2020; Kuchak et al., 2021). These innovations highlight the importance of material advancements and adaptive designs in modern transportation infrastructure.

The performance of asphalt mixtures can be further modified using various methods, including polymer and crumb rubber modifications. However, using such methods leads to increased costs for material and equipment procurement, thereby leading to the requirement of high budget allocations for highway agencies. An alternate option is to use recycled waste plastic material as a cost-effective and environmentally friendly option. Therefore, the use of polymethyl methacrylate derived from waste plastic can enhance the binder's performance in hot climatic conditions without compromising project costs.

Due to the constant increase in traffic volume and related axle loads, the use of conventional binder is not enough to sustain the pavement life for 10–15 years without modifying it with either Pmb or Crmb. Such an increase in traffic volume also requires the addition of maintenance interventions in pavement management systems, leading to high maintenance costs. The main purpose behind the usage of PMMA is to reduce maintenance costs without increasing the initial construction costs of the pavement.

Waste polymethyl methacrylate (PMMA) from stone-mastic asphalt was used in this study. Utilizing waste materials is crucial for improving the bitumen's properties and promoting sustainability in asphalt mixtures. Since the amount of plastic that is consumed in nature is growing at a rapid rate annually, plastic products are being produced at the same rate to meet this demand. Even though the recycling rate is only 12%, OECD reports predict that by 2060, the use of recycled plastics will exceed that of newly produced ones. This emphasizes recycling plastic.

One common kind of plastic is polymethyl methacrylate (PMMA), an amorphous polymer that is a member of the acrylic family. It is a methacrylate polymer with the chemical formula $C_5H_8O_2$. The production of PMMA is achieved through the polymerization of methyl methacrylate monomer. Methyl methacrylate polymerizes using methyl methacrylate monomer and an initiator (usually a peroxide). The polymerization process yields PMMA resin. It is commonly sold under commercial brands such as Plexiglas, Lucite, and Perspex. PMMA is transparent, translucent, or opaque, lightweight, durable, and chemically inert.

ITST (Indirect Tensile Strength Test) in the lab can be utilized to quantify and characterize the performance of modifiers based on resistance to fatigue damage (Xiao et al., 2018). Furthermore, the use of finite element modeling combined with the indirect tensile strength tests of different specimens can be employed to predict the fatigue damage performance of different asphalt mixtures.

ITST is employed in laboratories to evaluate the tensile strength properties of asphalt mixtures. Lab-prepared specimens can be used for indirect tensile strength testing and field core samples. Furthermore, cracking resistance and fatigue damage evaluation can also be performed using ITST (Dinis-Almeida et al., 2012). ITST can also be used to determine the moisture susceptibility of asphalt mixtures. In ITST, the cylindrical-shaped specimen is continuously loaded with a sinusoidal load pulse. The specimen is loaded at a speed of around 50 mm/min, and the maximum load at fracture is recorded (Li et al., 2017). ITST has also been previously used with the Marshall loading equipment with larger sample diameters of up to 150 mm to measure the Marshall stability as well as the optimum content of raw materials (Wang et al., 2018). ITST has also been used to evaluate the optimum amount of foamed asphalt for cold-in-place recycling techniques (Liu and Sun, 2023). It has been suggested that ITST be used in wet conditions to determine the optimum percentage of foamed asphalt (Kim and Lee, 2006). ITSM is another form of the indirect testing protocol for asphalt mixtures, where the stiffness modulus of asphalt mixtures is evaluated. ITSM is helpful for fatigue and rutting damage prediction of asphalt mixtures with temperature variations (Zhang et al., 2021). The stiffness modulus can also be determined using the indirect tensile stiffness modulus mode (ITSM) of the ITST, where the stiffness modulus is measured in a stress or strain-controlled mode using a series of vertical load impulses (Liu and Sun, 2023). For the ITSM tests, both laboratory-prepared specimens and field core specimens can be used. For ITSM tests, a rise time is specified, and a series of vertical load pulse applications are applied to measure the stiffness modulus of the specimen.

Meqtoof et al. (2024) performed an ITST test on a 5% SBS-modified specimen, using three different concentrations of ethylene butyl in the asphalt mixtures. Results suggested that the use of 2% ethylene butyl exhibited increased stability and indirect tensile strength. SBS specimens had 16% higher Marshall stability when compared to unmodified asphalt mixtures. Wang et al. (2017b) performed ITST and ITSM on different percentages of polymer-modified mixtures combined with neat asphalt mixtures to evaluate the capability of ITST and ITSM to differentiate different properties of polymer-modified and base asphalt mixtures.

Results showed that ITST was capable of evaluating the quality difference of core samples in terms of low-temperature cracking resistance. Although stiffness modulus increased in the case of SBS-modified mixtures, 13% higher loading cycles were required to reach the damage strains for the exact value of stiffness modulus for unmodified mixtures.

Wang et al. (2017a) evaluated the low-temperature performance of crumb rubber-modified asphalt mixtures using ITST and Semi-Circular Bending (SCB) tests. Different performance grade bitumen samples consisting of PG 64–22, PG 58–22 and neat PG 64–22 using 12% and 10% tire rubber were analyzed. Results showed increased low-temperature cracking resistance of CR-modified samples in the case of SCB testing. Furthermore, in the case of ITST, a 12% increase in tensile strength was observed for 58–22 binders with 12% tire rubber. It was found that the use of Advera and Evotherm type materials as external additives increased the low-temperature performance of asphalt mixtures (Wang et al., 2017a). In the case of the low-temperature cracking performance of polymer-modified asphalt mixtures, Du et al. (2020) evaluated different compositions of PE (Polyethylene) asphalt mixtures using ITST. The performance of the base asphalt mixture was evaluated against 3% PE and 4% PR-modified asphalt mixtures. The resulting tensile fatigue stress and strains were analyzed using ITST. Results showed adverse effects of using higher proportions of PE in bitumen samples in terms of increased crack size in samples. It was suggested to perform chemical modifications to PE-modified samples for further increase in low-temperature cracking resistance.

In terms of the use of finite element modeling, it has been previously used to evaluate the viscoelastic properties of asphalt mixtures in conjunction with lab tests. Huang et al. (2020) used finite element modeling to determine the stiffness modulus of damping asphalt mixtures and compared them against the indirect tension to cylindrical specimen test. Results concluded that the developed finite element model is capable of determining the viscoelastic properties of asphalt mixtures. Majidi Shad et al. (2022) used finite element modeling in conjunction with indirect tensile strength tests in the lab for asphalt mixtures with 50% and 80% RAP (Reclaimed Asphalt Pavement). Elastic and creep parameters were determined using indirect tensile strength tests and uniaxial repeated loading tests. Results showed the reasonable capability of the model to determine the rutting progression, with 50% and 80% RAP decreasing the rut depth by 33% and 47%, respectively. Yan et al. (2022) developed a model for the simulation of indirect tensile strength tests on asphalt mixtures with various thicknesses and layer compositions. Stress and strain responses at the bottom of the asphalt layer were measured, and the master curve was used to convert the relaxation modulus. Results showed that the interlayer tensile strain was highly dependent on the stiffer layer, and layers with high dynamic modulus have very little stress response. Furthermore, the developed finite element model showed a good correlation between simulated tensile stress and strain values and computed tensile stress and strain values in the lab.

## 2 Experimental

In this research, PMMA was used in proportions of 1%, 2%, 3%, 4% and 5% to SBS 3% binder. Samples were prepared with Marshal mix design and data with the addition of PMMA, and without PMMA in the case of base asphalt binder, they were recorded for penetration test, softening point test, Marshall stability and flow. Furthermore, experimental testing was performed to evaluate the indirect tensile strength and stiffness modulus of modified and base asphalt mixtures. Stiffness modulus tests were conducted at 1.2 Hz, 1.9 Hz, 3.9 Hz and 5 Hz. Indirect tensile strength was also measured at different loading rates from 10 MPa/s to 70 MPa/s with increments of 10 MPa/s. For damage distress evaluation, rutting and fatigue damage for each scenario was performed using the modified Burger's Logit model with finite element analysis in ABAQUS (Dassault Systèmes, 2021).

### 2.1 Material properties

Each mixture was categorized based on evaluated penetration and softening point properties. Penetration and softening points of each mixture were recorded and shown in Table 1.

Properties of aggregates based on aggregate quality testing are shown in Table 2. Various quality tests for aggregates in the lab, consisting of the Los Angeles abrasion test, Soundness test, test for Percentage of Flaky

**Table 1** ITST for variations ("*Q*" means "Penetration at 25 °C" [mm] according to ASTM International (2006a), hence "*S*" means "Softening point" [°C] according to ASTM International (2006b), "P." means "PMMA")

| | Base | SBS-7% | 1% P. | 2% P. | 3% P. | 4% P. | 5% P. |
|---|---|---|---|---|---|---|---|
| *Q* | 74.3 | 28 | 41 | 33 | 29 | 34 | 39 |
| *S* | 44.5 | 69 | 57 | 66 | 70 | 56 | 62 |

**Table 2** Aggregate properties

| Test | Unit | Standard | Result |
|---|---|---|---|
| Los Angeles Abrasion Test | % | EN 1097-2:2020 (CEN, 2020) | 20 |
| Fractured particles test | % | ASTM D5821-13 (ASTM International, 2017) | 91 |
| Aggregate soundness test | % | BS 812-121:1989 (BS Standards, 1989) | 6.5 |
| Friable particles test | % | ASTM C142/C142M-17 (ASTM International, 2023) | 1.2 |
| Flakiness index | % | EN 933-3:2012 (CEN, 2012) | 9 |

and elongated particles, test for percentage of fractured particles and test for percentage of friable particles, were conducted.

SBS is a commonly used polymer for asphalt mixtures due to enhancement in viscoelastic properties. SBS provides further resistance against permanent deformation at high temperatures and increased plasticity during low-temperature conditions, thereby creating a long-lasting asphalt mixture. The properties of SBS polymer are shown in Table 3.

PMMA is a clear, colorless polymer that has been used to further modify the SBS-based mixtures with a dosage of 1% to 5%. PMMA used in this research is sourced from Akipolymer. Further properties are shown in Table 4.

### 2.2 Indirect tensile strength testing

ITST was performed on the lab-prepared samples to evaluate the strength and modulus values. In the indirect tensile strength tests, the deformation rate is kept constant at 50.8 mm/min, and this test can be used to evaluate the fatigue cracking resistance of various asphalt mixtures.

Load application pattern is shown in Fig. 1 (CEN, 2018).

As observed, 1 is the peak load, 2 is the pulse repetition load, and 3 is the rise time. Loading is constantly increased until the specimen fractures, and the maximum load at that point is measured, as shown in Eq. (1) (CEN, 2018).

$$ITS = \frac{2P}{\pi Dt}, \tag{1}$$

where, *ITS* is the tensile strength in kPa, *P* is the peak load in N, and *D* and *t* are the diameter and thickness of the specimen in mm, respectively. Furthermore, the horizontal tensile strain was calculated for distress damage evaluation using Eq. (2).

$$\varepsilon_T = 13.2 H_T, \tag{2}$$

where, $\varepsilon_T$ is the horizontal tensile strain at fracture and $H_T$ is the horizontal deformation at peak load in mm. Four samples were prepared for each variation of base asphalt: 7% SBS, 3% SBS with 1% PMMA, 3% SBS with 2% PMMA, 3% SBS with 3% PMMA, 3% SBS with 4% PMMA and 3% SBS with 5% PMMA. Samples had a diameter of 100 mm and thickness of 45 mm, and they were compacted using a Marshall hammer with 75 blows and were prepared using ASTM D1559-89 (ASTM International, 1989). All the asphalt mixtures were prepared with a Marshall mix design. Since the stiffness of asphalt layers has a significant impact on the response to tensile strains at the bottom of asphalt layers to resist fatigue cracking, therefore, the stiffness modulus for the various asphalt mixtures is evaluated. The ITSM test is used to measure the stiffness moduli of the specimens with 15 load pulses in a 3 s duration of a sinusoidal waveform. Five subsequent pulses are used to determine the stiffness modulus of each mixture,

**Table 3** SBS properties

| Property | Unit | Value |
|---|---|---|
| Density | g/cm$^3$ | 0.89 |
| Flexural strength | GPa | 0.006 |
| Viscosity | cSt | 11–23 |
| Tensile strength | MPa | 9.5 |
| Linear mold shrinkage | cm/cm | 0.000–0.025 |

**Table 4** PMMA properties

| Property | Unit | Value |
|---|---|---|
| Density | g/cm$^3$ | 1.2 |
| Glass transition temperature range | °C | 100–130 |
| Water absorption | % | 0.3 |
| Linear shrinkage rate | cm/cm | 0.003–0.0065 |
| Linear mold shrinkage | cm/cm | 0.000–0.025 |

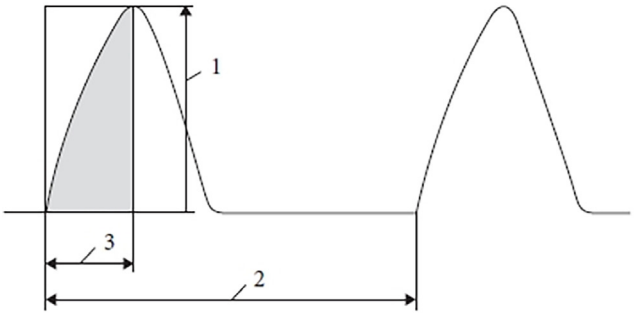


**Fig. 1** ITST schematic (CEN, 2018)

and the average value is calculated. The stiffness modulus is obtained from Eq. (3).

$$S_m = \frac{F \cdot (v + 0.27)}{z \cdot h}, \quad (3)$$

where, $S_m$ is the indirect tensile stiffness modulus in MPa, $F$ is the peak vertical load in N, $z$ is the average amplitude of 5 repeated horizontal deformations in mm, $h$ is the mean thickness of specimen in mm, and $v$ is the Poisson's ratio.

ITST was conducted as per CEN (2018) using COOPER HYD25 MKIII machine with pneumatic loading equipment using LVDT, as shown in Fig. 2. The ITST was conducted for samples of each variation, and results show the meaning of ITS values as shown in Table 5.

ITST, Marshall stability and Flow values are shown in Table 5. As observed, ITST and stability of PMMA samples increase with the increase in PMMA percentage, with a maximum strength of 2.028 MPa at 5% PMMA. A gradual increase in stability can also be observed with further addition of PMMA content. The performance of the PMMA-modified binder is significantly higher than that of base asphalt in terms of the indirect tensile strength achieved. Furthermore, the least flow is observed for 5% PMMA.

As observed in Fig. 3, the addition of PMMA helps the pavement resist significantly higher plastic strains and provides a prolonged pavement lifetime. SBS-7% performs slightly better than the 2% PMMA scenario. 5% PMMA provides 29% higher indirect tensile strength when compared to the base asphalt and around 22% higher performance when compared to 1% PMMA. Marshall stability further increases by 78% from base asphalt to 5% PMMA.

**Fig. 2** Cooper HYD 25 equipment

**Table 5** Marshall stability and flow

| ITST | Base | SBS-7% | PMMA | | | | |
|---|---|---|---|---|---|---|---|
| | | | 1% | 2% | 3% | 4% | 5% |
| MPa | 1.510 | 1.692 | 1.613 | 1.693 | 1.707 | 1.814 | 2.028 |
| Marshall Stability [kN] | 7.3 | 13.7 | 12.2 | 13.4 | 14.2 | 15.6 | 16.8 |
| Flow [mm] | 4.5 | 2.8 | 3.2 | 2.9 | 2.5 | 2.4 | 2.2 |

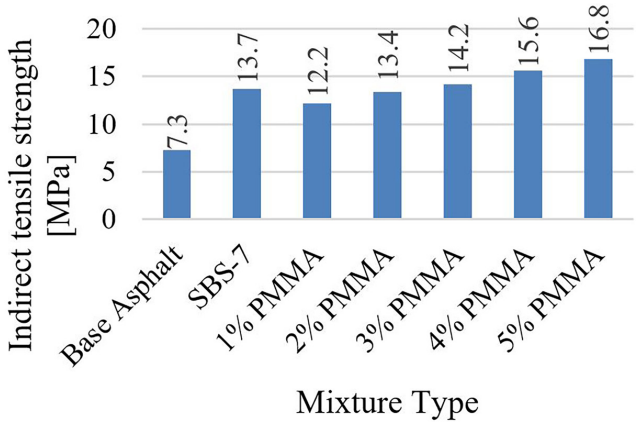


**Fig. 3** ITST results comparison

### 2.3 Stiffness modulus testing

The mean values of four samples prepared for each variation at a temperature of 20 °C with a load factor of 0.6 MPa are shown in (Fahad et al., 2021). Tests were continued as per CEN (2018) using a COOPER NU14 machine. As observed, the stiffness modulus increases with the added amount of PMMA. A 5% PMMA scenario yields an 18% higher stiffness modulus when compared to a 7% SBS. Furthermore, with an addition of only 1% PMMA to 3% SBS mixture, a 16% increase in stiffness modulus exists at 7.13 MPa when compared to that of base asphalt. PMMA modification performs better in terms of cohesion and production of a homogeneous mixture when compared to SBS only modified mixtures. Table 6 contains the stiffness moduli for all variations.

Furthermore, for the preparation of master curves, the stiffness moduli of the variations were evaluated with 4 different loading frequencies at 1.2 Hz, 1.9 Hz, 3.5 Hz and 5 Hz at 20 °C. These loading frequencies correspond

**Table 6** Stiffness moduli for all variations ("*U*" means "Load factor" [-], "*V*" means "Rise time" [ms], "*W*" means "Deformation" [mm], hence "*X*" is the "Stiffness modulus" [GPa])

| | Base | 7% SBS | PMMA with 3% SBS | | | | |
|---|---|---|---|---|---|---|---|
| | | | 1% | 2% | 3% | 4% | 5% |
| *U* | 0.4832 | 0.594 | 0.5714 | 0.5921 | 0.5963 | 0.5978 | 0.5989 |
| *V* | 123.4 | 125.3 | 122.6 | 124.1 | 123.5 | 124.3 | 123.7 |
| *W* | 0.0051 | 0.041 | 0.0048 | 0.0043 | 0.0041 | 0.0040 | 0.0039 |
| *X* | 6.05 | 7.71 | 7.13 | 7.64 | 7.96 | 7.67 | 8.61 |

to different instances of creep and rest cycles for evaluation of the elastic rebound of asphalt mixtures, which is usually measured in terms of stiffness modulus as an output. As the loading frequency increases from 1.2 Hz to 5 Hz, the rest period time is decreased by 25%, due to which less elastic rebound happens, and the resulting stiffness of the mixture increases significantly. This test indirectly characterizes the susceptibility of asphalt mixtures to fatigue damage at higher loading frequencies with small rest period durations. For each mixture variation, stiffness modulus was evaluated using the determination of continuous stress and strain values. For the development of master curves, the time-temperature superimposition principle has been used, as shown in Eq. (4) (Nguyen et al., 2013).

$$\log \propto_T = \frac{c_1 \cdot (T - T_{\text{ref}})}{c_2 + (T - T_{\text{ref}})}, \quad (4)$$

where, $\propto$ is the shift factor, $T$ is the testing temperature, $T_{\text{ref}}$ is the reference temperature, $C_1$ and $C_2$ are equation parameters. Furthermore, optimization of the shift factor is performed on the master curve, and the shift factor is applied to the phase angle master curve. Table 7 shows the stiffness modulus values for each mixture type corresponding to the loading frequencies of 1.2 Hz, 1.9 Hz, 3.5 Hz and 5 Hz. The base asphalt mixture yields a stiffness modulus of 6,953 MPa at 5 Hz, with the lowest stiffness modulus value at 6,103 MPa at 1.2 Hz compared to other mixtures. SBS 3% with 1% PMMA shows further improvement in the stiffness modulus when compared to the base asphalt, with a maximum stiffness modulus value of 7,212 MPa at 5 Hz. Improvement in increased stiffness modulus values continues with the addition of PMMA up to 5%, yielding a maximum stiffness modulus value of 8,741 MPa at 5 Hz · SBS.

### 2.4 ITS at various loading rates

A graphical representation of the comparison of stiffness modulus values at different frequencies is shown in Fig. 4. As observed, a gradual increase in stiffness modulus exists, with the highest stiffness modulus being shown by 3% SBS with 5% PMMA. SBS-7% shows identical performance to that of 3% SBS with 3% PMMA. SBS-7% shows a 12% increase in the stiffness modulus at 5 Hz when compared to base asphalt. 5% PMMA mixture shows a 10% higher stiffness modulus with a magnitude of 8,741 MPa at 5 Hz when compared to the SBS-7% scenario.

ITST was calculated for the mixture variations with an increment of loading rate from 10 MPa/s to 70 MPa/s, as shown in Table 8.

**Table 7** Stiffness modulus at variable frequencies

| Mixture type | Stiffness modulus [MPa] | Frequency [Hz] |
|---|---|---|
| Base asphalt | 6,953 | 5.0 |
| | 6,530 | 3.5 |
| | 6,280 | 1.9 |
| | 6,103 | 1.2 |
| SBS-7% | 7,851 | 5.0 |
| | 7,732 | 3.5 |
| | 7,531 | 1.9 |
| | 7,434 | 1.2 |
| SBS 3% with 1% PMMA | 7,515 | 5.0 |
| | 7,357 | 3.5 |
| | 7,246 | 1.9 |
| | 7,104 | 1.2 |
| SBS 3% with 2% PMMA | 7,840 | 5.0 |
| | 7,651 | 3.5 |
| | 7,422 | 1.9 |
| | 7,370 | 1.2 |
| SBS 3% with 3% PMMA | 8,052 | 5.0 |
| | 7,984 | 3.5 |
| | 7,824 | 1.9 |
| | 7,721 | 1.2 |
| SBS 3% with 4% PMMA | 8,131 | 5.0 |
| | 7,991 | 3.5 |
| | 8,031 | 1.9 |
| | 7,854 | 1.2 |
| SBS 3% with 5% PMMA | 8,741 | 5.0 |
| | 8,651 | 3.5 |
| | 8,502 | 1.9 |
| | 8,474 | 1.2 |

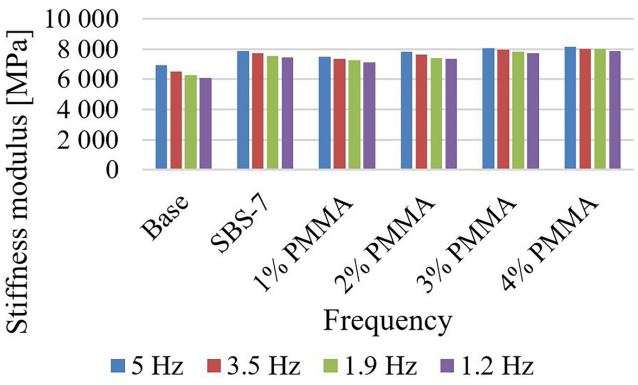


**Fig. 4** Stiffness modulus at variable frequencies

As observed from Table 8, indirect tensile strength gradually increases with the loading rate. A gradual increase in indirect tensile strength can be observed for base asphalt with 1.511 MPa at 10 MPa/s and a maximum strength of 3.482 MPa at 70 MPa/s. A similar pattern of increment

**Table 8** Indirect tensile strength at varying loading rates ("Base" means "Base asphalt", the abbreviation "P." means "PMMA")

| Loading rate [MPa/s] | Average strength [MPa] | | | | | | |
|---|---|---|---|---|---|---|---|
| | Base | 7% SBS | 1% P. | 2% P. | 3% P. | 4% P. | 5% P. |
| 10 | 1.511 | 1.691 | 1.603 | 1.67 | 1.709 | 1.802 | 2.012 |
| 20 | 2.281 | 2.483 | 2.421 | 2.456 | 2.552 | 2.595 | 2.652 |
| 30 | 2.713 | 2.974 | 2.880 | 2.924 | 3.037 | 3.090 | 3.158 |
| 40 | 2.976 | 3.297 | 3.161 | 3.208 | 3.331 | 3.391 | 3.463 |
| 50 | 3.190 | 3.510 | 3.386 | 3.441 | 3.571 | 3.633 | 3.713 |
| 60 | 3.376 | 3.698 | 3.584 | 3.641 | 3.781 | 3.845 | 3.931 |
| 70 | 3.482 | 3.796 | 3.696 | 3.753 | 3.897 | 3.965 | 4.052 |

in indirect tensile strength can be observed for PMMA-modified mixtures. SBS 3% with 5% PMMA exhibits the maximum indirect tensile strength when compared to other scenarios at all loading rates, with 2.012 MPa at 10 MPa/s and 4.052 MPa at 70 MPa/s.

As shown in Fig. 5, the 1% PMMA-modified mixture also performs significantly better than the base asphalt and yields 8% higher indirect tensile strength at a loading rate of 70 MPa/s, respectively. Identical performance in developed indirect tensile strength can be observed for both SBS-7% and SBS-3% with 3% PMMA mixtures.

## 3 Finite element modeling

The modified Burger Logit model was used for the simulation of each mixture type in finite element modeling software ABAQUS CAE 2023 (Dassault Systémes, 2023), as shown in Eq. (5).

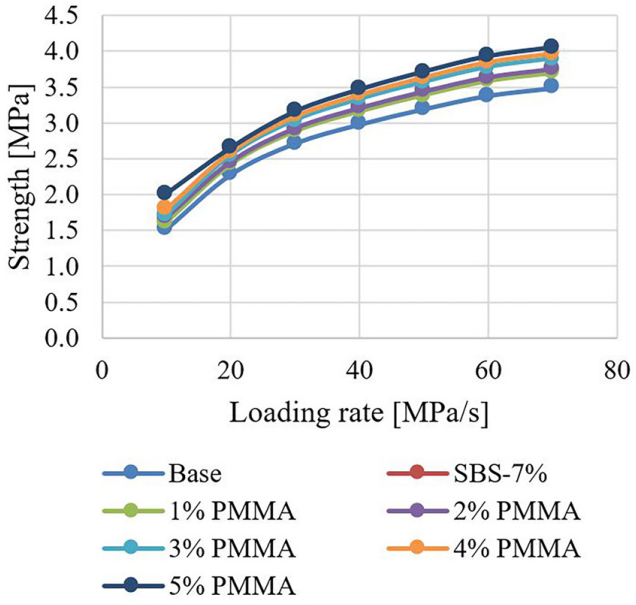


**Fig. 5** ITS at varying loading rates

$$\varepsilon(t)=\left[\frac{1}{E_0(1-\omega)}+\frac{1}{E_2}\left(1-e^{\frac{E_2}{n_2}}\right)+\frac{1}{A^{e^{BI}}}\right], \quad (5)$$

where $\varepsilon(t)$ is the creep strain of the modified Burgers model, $E_0$ is the dynamic modulus [MPa], $E_2$ is the internal damper parameter, $n_2$, $A$ and $B$ are the model viscoelastic fitted parameters, and $\omega$ is the damage value. The following creep parameters are considered for a temperature range of 30 °C in order to reduce the bias for significant increments in rutting magnitudes due to increased temperatures. These parameters improve the creep modeling capability by incorporating the creep development based on material decay using an external damper and external spring. Calculated material properties for each mixture type are shown in Table 9. As observed, parameter $A$ increases with the increase in PMMA content, with the highest magnitude of 165.63 MPa for a 5% PMMA mixture. Base asphalt exhibits the least magnitude of parameter $A$ at 102.57 MPa. Both SBS-7% and 3% PMMA show closer performance with magnitude of parameter $A$ at 156.14 MPa and 157.41 MPa.

In terms of loading, a dual wheel is used for loading propagation through the pavement structure. A commutative axle load of 100 kN is considered for a traffic volume of 50,000 axle passes at a speed of 90 km/h, as shown in Table 10.

A 2D finite element model has been created for properties taken from each mixture type. An asphalt layer with a thickness of 15 cm resting on a rigid foundation was assumed for microstrain analysis for all mixture types. The Visco step function was used to simulate the accurate deformation of the pavement under loading cycles. Cumulative loading time was used to simulate 50,000 passes with an

**Table 9** Burger's Logit model parameters

| Mixture type | $n_2$ [MPa] | $A$ [MPa] | $B$ | $R^2$ |
|---|---|---|---|---|
| Base asphalt | 3,431.45 | 102.57 | 0.000816 | 0.9902 |
| SBS-7% | 6,931.55 | 156.14 | 0.001045 | 0.9914 |
| SBS 3% with 1% PMMA | 6,563.54 | 149.25 | 0.001100 | 0.9907 |
| SBS 3% with 2% PMMA | 6,749.31 | 155.40 | 0.001048 | 0.9977 |
| SBS 3% with 3% PMMA | 7,031.25 | 157.41 | 0.001039 | 0.9928 |
| SBS 3% with 4% PMMA | 7,258.32 | 161.35 | 0.001049 | 0.9909 |
| SBS 3% with 5% PMMA | 7,725.48 | 165.63 | 0.001054 | 0.9989 |

**Table 10** Loading properties

| Tire type | Dual tire |
|---|---|
| Axle load | 100 kN |
| Ground pressure | 0.6 MPa |
| Number of axle passes | 50,000 |
| Speed | 90 km/h |
| Single loading time | 0.02149 s |
| Cumulative loading time | 11,524.33 s |

axle load of 100 kN. Results obtained from simulations were further used in fatigue and rutting damage analysis to yield the number of passes for fatigue and rutting damage. A convergence study was performed, and mesh size was adjusted at the optimum time and accuracy of results.

### 3.1 Model details

The model type used is a CPE4R model (Dassault Systémes, 2021) with reduced integration and hourglass control. The total number of elements is 6,100, with an element size of 5 mm for increased accuracy after the convergence study. As observed from Fig. 6, movement along the normal vertical directions is allowed; however, movements along the horizontal directions are restricted. Both axes follow asymmetric restrictions in horizontal and vertical directions along the rigid foundation to reduce any bias in terms of evaluated principal stress and strain values. These boundary conditions were used to allow for accurate deformation and evaluation of limit strains along normal vertical directions.

### 3.2 Simulation results

Simulations for each mixture type were performed for a total of 50,000 passes in ABAQUSCAE 2023 (Dassault Systémes, 2023). Deformation results for the 3% SBS with 1% PMMA mixture are shown in Fig. 7.

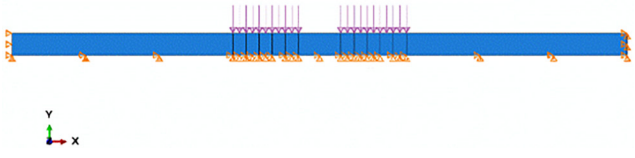

**Fig. 6** Loading and boundary conditions details

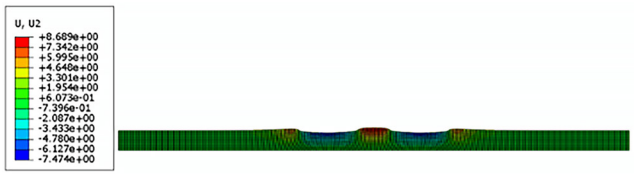


**Fig. 7** Simulation results for SBS-3% with 3% PMMA

As observed, rutting and upheaval sections can be observed along the tire paths, with deformations clearly visible. Simulations for each mixture were conducted with red-colored portions corresponding to upheaval and blue-colored portions corresponding to the resulting rut increment.

Furthermore, Von Mises stress values for each mixture type were calculated based on individual corresponding $n_2$, $A$ and $B_t$ parameters. Base asphalt exhibits the highest rutting magnitude among other scenarios, with the least rutting magnitude exhibited by 3% SBS and 5% PMMA. SBS-7% shows better rutting performance than 2% PMMA with 3% SBS mixtures.

The Von Mises stress values for each mixture type are shown in (Fahad et al., 2024). Measurement depths are 50 mm, 450 mm and 800 mm. Stress concentration gradually decreases from 50 mm to 800 mm. SBS-3% with 4% and 5% PMMA show the lowest stress concentrations. SBS-7% and SBS-3% with 3% PMMA exhibit almost identical stress concentrations. However, base asphalt exhibits higher stress concentrations from 50 mm to 800 mm.

The use of PMMA for SBS-modified mixtures further decreases stress concentrations, leading to increased resistance against rutting. Table 11 gives Von Mises values.

## 4 Fatigue and rutting damage analysis

The fatigue life of the pavement can be measured in the number of passes to cause fatigue damage. Furthermore, the number of passes that cause permanent deformation can also be evaluated. Usually, permanent deformation occurs as a result of densification and shear deformation of the pavement under load and increased temperature conditions. The Asphalt Institute model provides the relationship between fatigue life and resulting horizontal tensile strains at the bottom of the asphalt layer using Eq. (6) (Zhou et al., 2007).

$$N_f = 0.0796 \cdot \varepsilon_t^{-3.291} \cdot E^{-0.854}, \tag{6}$$

where, $N_f$ is the number of load repetitions to fatigue damage, $\varepsilon_t$ is the horizontal tensile strain at the bottom of the asphalt layer, $E$ is the elastic modulus of the asphalt mixture. The relationship between the compressive strain and

**Table 11** Von Mises values

| Dep. [mm] | Base | SBS-7% | PMMA | | | | |
|---|---|---|---|---|---|---|---|
| | | | 1% | 2% | 3% | 4% | 5% |
| 50 | 2.97 | 2.30 | 2.46 | 2.31 | 2.30 | 2.33 | 2.58 |
| 450 | 0.31 | 0.25 | 0.27 | 0.26 | 0.24 | 0.26 | 0.23 |
| 800 | 0.071 | 0.023 | 0.025 | 0.024 | 0.023 | 0.025 | 0.022 |

rutting damage is provided by the Asphalt Institute model using Eq. (7) (Asphalt Institute, 1982).

$$N_f = 1.365 \cdot 10^{-9} \cdot \varepsilon_c^{-4.477}, \quad (7)$$

where, $N_f$ is the number of load repetitions to rutting damage and $\varepsilon_c$ is the vertical compressive strain on top of the subgrade. In terms of evaluation of the design life of pavement based on the number of repetitions to fatigue and rutting damage, the incremental damage can be used to evaluate the damage factor of all the axle loads over the pavement lifetime, as shown in Eq. (8).

$$D_f = \sum \frac{N_i}{N_r}, \quad (8)$$

where, $D_f$ is the damage factor, $N_i$ is the actual number of load repetitions and $N_r$ is the number of load repetitions to fatigue or rutting damage. Fahad and Nagy (2023) show the resulting strain values obtained from simulations along with the loading repetitions to fatigue and rutting damage. As observed, the number of repetitions to fatigue and rutting damage increases with the increase in PMMA content. The addition of 5% PMMA to 3% SBS further enhances the fatigue and rutting durability of the mixture, yielding up to $8.11 \cdot 10^6$ number of passes to fatigue damage and $7.64 \cdot 10^{10}$ passes to rutting damage. Base asphalt exhibits the lowest number of passes to damage, with fatigue number at $5.80 \cdot 10^9$ passes and rutting number at $0.96 \cdot 10^6$ passes. Consequently, the least strain magnitude is observed under modification with PMMA for scenarios from 1% to 5% PMMA modification.

As observed from Fig. 8, the highest number of passes to fatigue damage is shown by the 5% PMMA with 3% SBS mixture at $7.75 \cdot 10^{10}$ passes. The least number of passes exist for base asphalt at $1.80 \cdot 10^{10}$ passes. Furthermore, the 5% PMMA mixture exhibits an overall 21% higher number of passes to fatigue damage when compared to the SBS-7% mixture. A closer difference in the number of fatigue passes for both SBS-7% and PMMA 3% can be observed.

Table 12 represents the compressive and tensile strains for all variations.

A graphical representation of rutting performance for each scenario is shown in Fig. 9. As observed, the highest rutting accumulation is shown by base asphalt with the least number of passes at $0.96 \cdot 10^6$ passes. The highest rutting performance is exhibited by the 5% PMMA scenario, with the maximum number of passes at $8.11 \cdot 10^6$. Almost identical performance can be observed for both SBS-7% and PMMA 3% mixtures with $6.38 \cdot 10^6$ and $6.48 \cdot 10^6$ passes to rutting damage.

## 5 Conclusions

In this research, SBS-modified asphalt mixtures were treated with various percentages of PMMA ranging from

**Table 12** Compressive and tensile strains for all variations

| Mixture type | Strain types | Value [Microns] | Number of passes to damage |
|---|---|---|---|
| Base asphalt | $\varepsilon_t$ | 36.1 | $1.80 \cdot 10^{10}$ |
| | $\varepsilon_c$ | 541.7 | $0.96 \cdot 10^6$ |
| SBS-7% | $\varepsilon_t$ | 22.4 | $6.24 \cdot 10^{10}$ |
| | $\varepsilon_c$ | 453.1 | $6.38 \cdot 10^6$ |
| SBS 3% with 1% PMMA | $\varepsilon_t$ | 28.9 | $3.96 \cdot 10^{10}$ |
| | $\varepsilon_c$ | 484.3 | $2.78 \cdot 10^6$ |
| SBS 3% with 2% PMMA | $\varepsilon_t$ | 26.8 | $5.86 \cdot 10^{10}$ |
| | $\varepsilon_c$ | 478.3 | $4.50 \cdot 10^6$ |
| SBS 3% with 3% PMMA | $\varepsilon_t$ | 20.3 | $7.01 \cdot 10^{10}$ |
| | $\varepsilon_c$ | 450.2 | $6.48 \cdot 10^6$ |
| SBS 3% with 4% PMMA | $\varepsilon_t$ | 24.0 | $7.41 \cdot 10^{10}$ |
| | $\varepsilon_c$ | 456.3 | $7.12 \cdot 10^6$ |
| SBS 3% with 5% PMMA | $\varepsilon_t$ | 18.3 | $7.75 \cdot 10^{10}$ |
| | $\varepsilon_c$ | 440.9 | $8.11 \cdot 10^6$ |

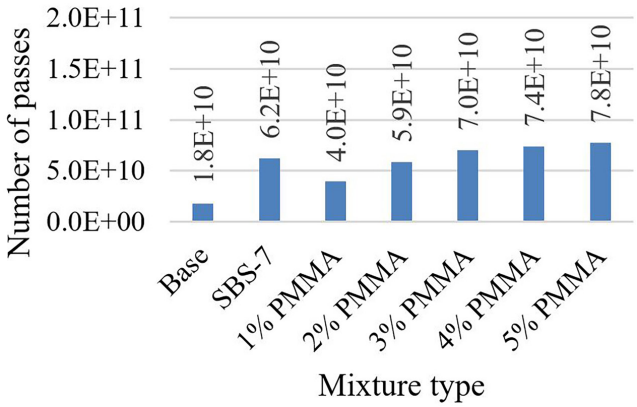


**Fig. 8** Comparison of number of passes to fatigue damage

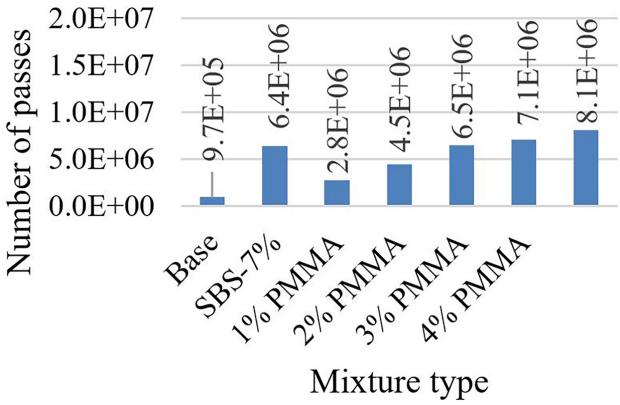


**Fig. 9** Comparison of number of passes to rutting damage

1% to 5% PMMA added to 3% SBS-modified asphalt mixture. Furthermore, a comparison was made with an asphalt mixture with SBS-7% only in terms of indirect tensile strength tests and stiffness modulus tests. Stiffness modulus tests were performed for all scenarios under varying loading frequencies of 5 Hz, 3.5 Hz, 1.9 Hz and 1.2 Hz.

Moreover, various loading rates were applied during indirect tensile strength measurements from 10 MPa/s to 70 MPa/s to measure the deformation resistance of various samples. Finite element modeling was further performed using the modified Burger's Logit model, where the rutting and fatigue number of passes for each mixture variation were evaluated. The addition of PMMA to SBS-modified mixtures further enhances the viscoelastic properties and operational temperature range of the mixtures. Mixtures were modified with 1%–5% PMMA added to 3% SBS.

The addition of PMMA to asphalt mixtures improves the cohesion and deformation resistance all the way to 5% PMMA. The use of 5% PMMA is recommended for SBS-modified asphalt mixtures since it provides a cost-effective alternative against the usage of 7% SBS only asphalt mixtures. The findings are as follows.

1. PMMA-modified mixtures perform better than the conventional SBS only modified mixtures, yielding higher stiffness modulus at higher temperatures.
2. SBS-3% with PMMA 5% provides the best performance in terms of reduced permanent deformation, showing overall 12.6% superior performance when compared to base asphalt mixture and 6.8% better performance when compared to SBS-7%.
3. SBS-3% with PMMA 4% performs 7.5% better than the PMMA 1% mixture, showing a gradual reduction in the progression of fatigue damage.
4. In terms of rutting performance, PMMA 5% supersedes SBS-7% by 6.2%, PMMA 4% by 4.9% and base asphalt mixture by 16%.
5. Based on the availability and cost of PMMA, the dosage of 3% and 4% PMMA to conventional SBS-3% modified asphalt mixtures can provide promising results and outperform the SBS only modified asphalt mixtures.
6. SBS-7% and SBS 3% with 3% PMMA show closer performance in terms of indirect tensile strength and stiffness modulus values.

Future research should focus on addressing accurate material models and sophisticated FE models. Such studies would provide critical insights into preventing premature structural failure and deformations, possibly applying artificial intelligence or learning algorithms (Nosonovsky and Aglikov, 2024; Zamfirache et al., 2023), big data usage (Lekić et al., 2021), optimization techniques (Fischer and Kocsis Szürke, 2023; Mzili et al., 2023; Zalacko et al., 2020), further field tests and laboratory examinations (Liović et al., 2024; Zheng and Wang, 2024), considering cognitive mobility concept (Zöldy et al., 2024; Zöldy and Baranyi, 2023), etc.

It is worth conducting research on the long-term behavior of the PMMA and SBS-modified bitumens and the asphalt mixtures produced using them, like Li et al. (2022), Li et al. (2023), Li et al. (2024), as well as Mo (2023). Fahad et al. (2024) executed FE simulations in ABAQUS CAE 2023 (Dassault Systémes, 2023); however, the laboratory tests and field tests would be of more benefit to be able to determine the empirical and fundamental characteristics of these mixtures and pavements in a more detailed manner.

**Acknowledgement**

This paper was prepared by the research team "SZE-RAIL". This research was supported by SIU Foundation's project, Sustainable railways – Investigation of the energy efficiency of electric rail vehicles and their infrastructure'. The publishing of the paper did not receive financial support or financing of the article process charge.

**List of abbreviations**

| | |
|---|---|
| AI | Artificial Intelligence |
| ASTM | American Society for Testing and Materials |
| BS | British Standards |
| CEN | European Committee for Standardization |
| CR | Crumb Rubber |
| EN | European Norm |
| FE | Finite Element |
| ITSM | Indirect Tensile Stiffness Modulus |
| ITST | Indirect Tensile Strength Test |
| LVDT | Linear Variable Differential Transformer |
| OECD | Organization for Economic Co-operation and Development |
| PE | Polyethylene |
| PMB | Polymer Modified Bitumen |
| PMMA | Polymethyl Methacrylate |
| RAP | Reclaimed Asphalt Pavement |
| SBS | Styrene-Butadiene-Styrene |
| SCB | Semi-Circular Bending Test |

## List of symbols

| Symbol | Meaning | Unit |
|---|---|---|
| $\alpha$ | Shift factor according to CEN (2018) | - |
| $A$ | Model viscoelastic fitted parameters of the modified Burgers model according to Dassault Systèmes (2021) | - |
| $B$ | Model viscoelastic fitted parameters of the modified Burgers model according to Dassault Systèmes (2021) | - |
| $C_1$ | Equation parameter according to CEN (2018) | - |
| $C_2$ | Equation parameter according to CEN (2018) | - |
| $D$ | Diameter of the specimen according to CEN (2018) | mm |
| $D_f$ | Damage factor | - |
| $E$ | Elastic modulus of the asphalt mixture according to Zhou et al. (2007) | MPa |
| $e(t)$ | Creep strain of the modified Burgers model according to Dassault Systèmes (2021) | - |
| $E_0$ | Dynamic modulus of the modified Burgers model according to Dassault Systèmes (2021) | MPa |
| $E_2$ | Internal damper parameter of the modified Burgers model according to Dassault Systèmes (2021) | - |
| $\varepsilon_c$ | Vertical compressive strain on top of the subgrade according to Asphalt Institute (1982) | - |
| $\varepsilon_t$ | Horizontal tensile strain at fracture according to ASTM International (1989) | - |
| $\varepsilon_t$ | Horizontal tensile strain at the bottom of the asphalt layer according to Zhou et al. (2007) | - |
| $h$ | Mean thickness of the specimen according to CEN (2018) | mm |
| $H_t$ | Horizontal deformation at peak load according to ASTM International (1989) | mm |
| $ITS$ | Tensile strength according to CEN (2018) | kPa |
| $\nu$ | Poisson's ratio according to CEN (2018) | - |
| $n_2$ | Model viscoelastic fitted parameters of the modified Burgers model according to Dassault Systèmes (2021) | - |
| $N_f$ | Number of load repetitions to fatigue damage of von Mises stresses according to Dassault Systèmes (2021) | - |
| $N_i$ | Actual number of load repetitions in fatigue and rutting damage analysis | - |
| $N_i$ | Number of load repetitions to fatigue or rutting damages in fatigue and rutting damage analysis | - |
| $P$ | Peak load according to CEN (2018) | N |
| $Q$ | Penetration at 25 °C according to ASTM International (2006a) | mm |
| $S$ | Softening point according to ASTM International (2006b) | °C |
| $S_m$ | Indirect tensile stiffness modulus according to CEN (2018) | MPa |
| $t$ | Thickness of the specimen according to CEN (2018) | mm |
| $T$ | Testing temperature according to CEN (2018) | °C |
| $T_r$ | Reference temperature according to CEN (2018) | °C |
| $U$ | Load factor according to CEN (2018) | - |
| $V$ | Rise time according to CEN (2018) | ms |
| $W$ | Deformation according to CEN (2018) | mm |
| $\omega$ | Damage value of the modified Burgers model according to Dassault Systèmes (2021) | - |
| $X$ | Stiffness modulus according to CEN (2018) | GPa |
| $z$ | Average amplitude of 5 repeated horizontal deformations according to CEN (2018) | mm |

## References

Asphalt Institute (1982) "Research and development of the asphalt institute's thickness design manual (MS-1) ninth edition", The Asphalt Institute, Lexington, KY, USA, (RR-82-2).

ASTM International (1989) "ASTM D1559-89 Standard test method for resistance to plastic flow of bituminous mixtures using Marshall apparatus", American Society for Testing and Materials, West Conshohocken, PA, USA.

ASTM International (2006a) "ASTM D5-06e1 Standard test method for penetration of bituminous materials", American Society for Testing and Materials, West Conshohocken, PA, USA.

ASTM International (2006b) "ASTM D36-06 Standard test method for softening point of bitumen (ring-and-ball apparatus)", American Society for Testing and Materials, West Conshohocken, PA, USA.

ASTM International (2017) "ASTM D5821-13 Standard test method for determining the percentage of fractured particles in coarse aggregate", American Society for Testing and Materials, West Conshohocken, PA, USA.

ASTM International (2023) "ASTM C142/C142M-17 Standard test method for clay lumps and friable particles in aggregates", American Society for Testing and Materials, West Conshohocken, PA, USA. https://doi.org/10.1520/C0142_C0142M-17

BS Standards (1989) "BS 812-121:1989 Testing aggregates. Method for determination of soundness", British Standards Institution, London, UK.

CEN (2012) "EN 933-3:2012 Tests for geometrical properties of aggregates – Part 3: Determination of particle shape – Flakiness index", European Committee for Standardization, Brussels, Belgium.

CEN (2018) "EN 12697-26:2018 Bituminous mixtures – Test methods – Part 26: Stiffness", European Committee for Standardization, Brussels, Belgium.

CEN (2020) "EN 1097-2:2020 Tests for mechanical and physical properties of aggregates – Part 2: Methods for the determination of resistance to fragmentation", European Committee for Standardization, Brussels, Belgium.

Dassault Systèmes (2021) "Abaqus 2021 documentation", Dassault Systèmes Simulia Corporation, Providence, RI, USA.

Dassault Systèmes (2023) "Abaqus 2023 documentation", Dassault Systèmes Simulia Corporation, Providence, RI, USA.

Dinis-Almeida, M., Castro-Gomes, J., Antunes, M. D. L. (2012) "Mix design considerations for warm mix recycled asphalt with bitumen emulsion", Construction and Building Materials, 28(1), pp. 687–693. https://doi.org/10.1016/j.conbuildmat.2011.10.053

Du, Z., Jiang, C., Yuan, J., Xiao, F., Wang, J. (2020) "Low temperature performance characteristics of polyethylene modified asphalts – A review", Construction and Building Materials, 264, 120704. https://doi.org/10.1016/j.conbuildmat.2020.120704

Ézsiás, L., Tompa, R., Fischer, S. (2024) "Investigation of the possible correlations between specific characteristics of crushed stone aggregates", Spectrum of Mechanical Engineering and Operational Research, 1(1), pp. 10–26. https://doi.org/10.31181/smeor1120242

Fahad, M., Koren, C., Nagy, R. (2024) "Finite element modelling of polymer and crumb rubber modified asphalt mixtures", Material Strength and Applied Mechanics, 59, pp. 44–52. https://doi.org/10.3233/ATDE240525

Fahad, M., Nagy, R. (2023) "Effective lane width analysis for autonomous trucks", SN Applied Sciences, 5(9), 232. https://doi.org/10.1007/s42452-023-05446-0

Fahad, M., Nagy, R., Füleki, P. (2021) "Creep model to determine rut development by autonomous truck axles on pavement", Pollack Periodica, 17(1), pp. 66–71. https://doi.org/10.1556/606.2021.00328

Fischer, S. (2025) "Investigation of the settlement behavior of ballasted railway tracks due to dynamic loading", Spectrum of Mechanical Engineering and Operational Research, 2(1), pp. 24–46. https://doi.org/10.31181/smeor21202528

Fischer, S., Kocsis Szürke, S. (2023) "Detection process of energy loss in electric railway vehicles", Facta Universitatis, Series: Mechanical Engineering, 21(1), pp. 81–99. https://doi.org/10.22190/FUME221104046F

Huang, J., Duan, T., Sun, Y., Wang, L., Lei, Y. (2020) "Finite element (FE) modeling of indirect tension to cylindrical (IT-CY) specimen test for damping asphalt mixtures (DAMs)", Advances in Civil Engineering, 2020(1), 6694180. https://doi.org/10.1155/2020/6694180

Kim, Y., Lee, H. D. (2006) "Development of mix design procedure for cold in-place recycling with foamed asphalt", Journal of Materials in Civil Engineering, 18(1), pp. 116–124. https://doi.org/10.1061/(asce)0899-1561(2006)18:1(116)

Kuchak, A. J. T., Marinkovic, D., Zehn, M. (2020) "Finite element model updating – Case study of a rail damper", Structural Engineering and Mechanics, 73(1), pp. 27–35. https://doi.org/10.12989/sem.2020.73.1.027

Kuchak, A. J. T., Marinkovic, D., Zehn, M. (2021) "Parametric investigation of a rail damper design based on a lab-scaled model", Journal of Vibration Engineering and Technologies, 9(1), pp. 51–60. https://doi.org/10.1007/s42417-020-00209-2

Lekić, M., Rogić, K., Boldizsár, A., Zöldy, M., Török, Á. (2021) "Big data in logistics", Periodica Polytechnica Transportation Engineering, 49(1), pp. 60–65. https://doi.org/10.3311/PPTR.14589

Li, R., Xiao, F., Amirkhanian, S., You, Z., Huang, J. (2017) "Developments of nano materials and technologies on asphalt materials – A review", Construction and Building Materials, 143, pp. 633–648. https://doi.org/10.1016/j.conbuildmat.2017.03.158

Li, Y., Yan, X., Guo, J., Wu, W., Shi, W., Xu, Q., Ji, Z. (2023) "Performance and verification of high-modulus asphalt modified by styrene-butadiene-styrene block copolymer (SBS) and rock asphalt", Coatings, 13(1), 38. https://doi.org/10.3390/coatings13010038

Li, H., Wang, H., Lin, J., Yang, J., Yao, Y. (2024) "Study on the effect of SBS/HVA/CRM composite-modified asphalt on the performance of recycled asphalt mixtures", Polymers, 16(22), 3226. https://doi.org/10.3390/polym16223226

Liović, D., Franulović, M., Ferlič, L., Gubeljak, N. (2024) "Surface roughness of Ti6Al4V alloy produced by laser powder bed fusion", Facta Universitatis, Series: Mechanical Engineering, 22(1), pp. 63–76. https://doi.org/10.22190/FUME230719030L

Liu, Z., Sun, L. (2023) "A review of effect of compaction methods on cold recycling asphalt mixtures", Construction and Building Materials, 401, 132758. https://doi.org/10.1016/j.conbuildmat.2023.132758

Majidi Shad, M. M., Khabiri, M. M., Arabani, M., Bahmani, H. (2022) "3D finite element model for recycled asphalt mixtures with high percentages of reclaimed asphalt pavement rutting simulation", International Journal of Engineering, Transactions A: Basics, 35(7), pp. 1428–1439. https://doi.org/10.5829/ije.2022.35.07a.20

Meqtoof, F. H., Aodah, H. H., Naser, I. H., Ali, A. H. M. (2024) "Evaluation of compressive strength of asphalt mixture from marshall stability and indirect tensile strength", Mathematical Modelling of Engineering Problems, 11(6), pp. 1473–1480. https://doi.org/10.18280/mmep.110608

Mo, Z. (2023) "Study on the performance and aging low temperature performance of GO / SBS modified asphalt", Matéria (Rio de Janeiro), 28(3), e20230151. https://doi.org/10.1590/1517-7076-rmat-2023-0151

Mzili, T., Mzili, I., Riffi, M. E., Pamucar, D., Simic, V., Kurdi, M. (2023) "A novel discrete rat swarm optimization algorithm for the quadratic assignment problem", Facta Universitatis, Series: Mechanical Engineering, 21(3), pp. 529–552. https://doi.org/10.22190/FUME230602024M

Nagy, R., Horvát, F., Fischer, S. (2024) "Innovative approaches in railway management: Leveraging big data and artificial intelligence for predictive maintenance of track geometry", Tehnički Vjesnik, 31(4), pp. 1245–1259. https://doi.org/10.17559/TV-20240420001479

Nguyen, M. L., Sauzéat, C., Di Benedetto, H., Tapsoba, N. (2013) "Validation of the time-temperature superposition principle for crack propagation in bituminous mixtures", Materials and Structures, (Materiaux et Constructions), 46(7), pp. 1075–1087. https://doi.org/10.1617/s11527-012-9954-7

Nosonovsky, M., Aglikov, A. S., (2024) "Triboinformatics: machine learning methods for frictional instabilities", Facta Universitatis, Series: Mechanical Engineering, 22(3), pp. 423–433. https://doi.org/10.22190/FUME231208013N

Saukenova, I., Oliskevych, M., Taran, I., Toktamyssova, A., Aliakbarkyzy, D., Pelo, R. (2022) "Optimization of schedules for early garbage collection and disposal in the megapolis", Eastern-European Journal of Enterprise Technologies, 1(3(115)), pp. 13–23. https://doi.org/10.15587/1729-4061.2022.251082

Vitković, N., Marinković, D., Stan, S. D., Simonović, M., Miltenović, A., Tomić, M., Barać, M. (2024) "Decision support system for managing marshalling yard deviations", Acta Polytechnica Hungarica, 21(1), pp. 121–134. https://doi.org/10.12700/APH.21.1.2024.1.8

Volkov, V., Taran, I., Volkova, T., Pavlenko, O., Berezhnaja, N. (2020) "Determining the efficient management system for a specialized transport enterprise", Naukovyi Visnyk Natsionalnoho Hirnychoho Universytetu, 4, pp. 185–191. https://doi.org/10.33271/nvngu/2020-4/185

Wang, T., Xiao, F., Amirkhanian, S., Huang, W., Zheng, M. (2017a) "A review on low temperature performances of rubberized asphalt materials", Construction and Building Materials, 145, pp. 483–505. https://doi.org/10.1016/j.conbuildmat.2017.04.031

Wang, T., Xiao, F., Zhu, X., Huang, B., Wang, J., Amirkhanian, S. (2018) "Energy consumption and environmental impact of rubberized asphalt pavement", Journal of Cleaner Production, 180, pp. 139–158. https://doi.org/10.1016/j.jclepro.2018.01.086

Wang, Y., Chong, D., Wen, Y. (2017b) "Quality verification of polymer-modified asphalt binder used in hot-mix asphalt pavement construction", Construction and Building Materials, 150, pp. 157–166. https://doi.org/10.1016/j.conbuildmat.2017.05.196

Xiao, F., Yao, S., Wang, J., Li, X., Amirkhanian, S. (2018) "A literature review on cold recycling technology of asphalt pavement", Construction and Building Materials, 180, pp. 579–604. https://doi.org/10.1016/j.conbuildmat.2018.06.006

Yan, K., Wang, S., Ge, D., Chen, J., Tian, S., Sun, H. (2022) "Laboratory performance of asphalt mixture with waste tyre rubber and APAO modified asphalt binder", International Journal of Pavement Engineering, 23(1), pp. 59–69. https://doi.org/10.1080/10298436.2020.1730837

Zalacko, R., Zöldy, M., Simongáti, G. (2020) "Comparative study of two simple marine engine BSFC estimation methods", Brodogradnja: An International Journal of Naval Architecture and Ocean Engineering for Research and Development, 71(3), pp. 13–25. https://doi.org/10.21278/brod71302

Zamfirache, I. A., Precup, R.-E., Petriu, E. M. (2023) "Q-learning, policy iteration and actor-critic reinforcement learning combined with metaheuristic algorithms in servo system control", Facta Universitatis, Series: Mechanical Engineering, 21(4), pp. 615–630. https://doi.org/10.22190/FUME231011044Z

Zhang, J., Zheng, M., Xing, X., Pei, J., Zhang, J., Li, R., Xu, P., Wang, D. (2021) "Investigation on the designing method of asphalt emulsion cold recycled mixture based on one-time compaction", Journal of Cleaner Production, 286, 124958. https://doi.org/10.1016/j.jclepro.2020.124958

Zheng, J., Wang, L. (2024) "Experimental study on creep loading of porous coal under different influencing factors", Facta Universitatis, Series: Mechanical Engineering, 22(1), pp. 153–163. https://doi.org/10.22190/FUME2312050l1Z

Zhou, F., Fernando, E., Scullion, T. (2007) "A review of performance models and test procedures with recommendations for use in the texas M-E design program 5", Texas Transportation Institute, Austin, Texas, USA, (Rep. 0-5798-1).

Zöldy, M., Baranyi, P. (2023) "The cognitive mobility concept", Infocommunications Journal, 15, pp. 35–40. https://doi.org/10.36244/ICJ.2023.SI-IODCR.6

Zöldy, M., Baranyi, P., Török, Á. (2024) "Trends in cognitive mobility in 2022", Acta Polytechnica Hungarica, 21(7), pp. 189–202. https://doi.org/10.12700/APH.21.7.2024.7.11